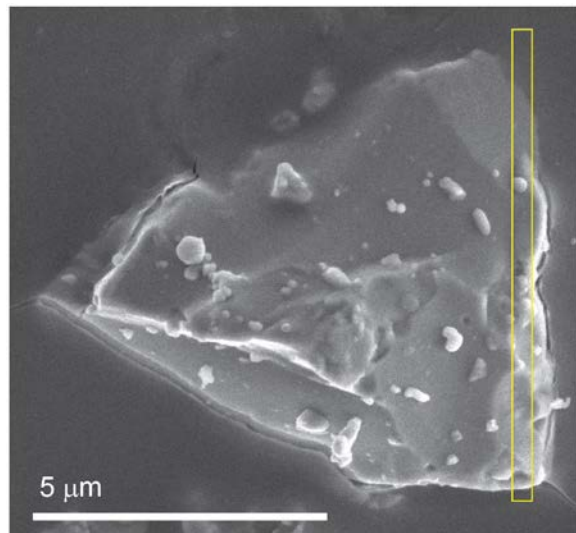


**WATER IN VESICLES IN SPACE WEATHERED RIM OF LUNAR APATITE.** K.D. Burgess<sup>1</sup> and R.M. Stroud<sup>1</sup>, <sup>1</sup>U.S. Naval Research Laboratory, 4555 Overlook Ave. SW, Washington, DC 20375 USA (kate.burgess@nrl.navy.mil).

**Introduction:** Apatite ( $\text{Ca}_5(\text{PO}_4)_3(\text{F}, \text{Cl}, \text{OH})$ ) is present in minor amounts on many Solar System bodies, including the Moon, where it is the most common naturally water-bearing phase [1]. The ability of apatite to contain and retain water in its crystal structure makes it unique among lunar minerals. Its low abundance compared to the main silicate phases means its response to space weathering has not been studied.

Irradiation by the solar wind leads to alteration and often amorphization of the very surface of exposed materials [2]. Hydrogen and helium, the most abundant ions in the solar wind, can be trapped within the irradiated rim, potentially forming vesicles the contents of which can be analyzed using electron energy loss spectroscopy (EELS) in the transmission electron microscope (TEM) [3,4]. The formation of these vesicles could affect lunar water cycling, exosphere composition, and access to these volatiles for in situ resource utilization (ISRU) [5,6]. However, in situ measurements of H or  $\text{H}_2\text{O}$  within lunar space weathered rim material that can be definitively separated from terrestrial contamination have not yet been reported. We report the clear presence of water in vesicles in a space weathered lunar apatite grain.



**Figure 1.** SEM image of a lunar apatite grain mounted in epoxy. Yellow box indicates location of FIB section.

**Methods:** The apatite grain is from mature lunar soil 79221 ( $\text{I}/\text{FeO} = 81$ ). The particle was mounted in epoxy such that one surface of the grain was available for imaging in the SEM. FIB samples were prepared

with an FEI Helios G3 equipped with an Oxford 150  $\text{mm}^2$  SDD energy dispersive X-ray spectrometer (EDS). After imaging, protective straps of C were deposited on regions of interest, first with e-beam then i-beam. A section suitable for STEM analysis was extracted using standard techniques and mounted on a Cu half-grid. STEM analysis was performed with the Nion UltraSTEM200-X at NRL. The microscope is equipped with a Gatan Enfium ER spectrometer for EELS and a windowless, 0.7 sr Bruker SDD-EDS detector. Data were collected at 200 kV.

**Results and Discussion:** The prepared apatite sample is  $\sim 6.5 \times 1.5 \mu\text{m}$  with a significant portion of the grain surface on multiple sides being available for study. Space weathering varies between the top and bottom as it was mounted in the epoxy. EDS shows the apatite is F-rich, and assuming  $\text{F} + \text{Cl} + \text{OH} = 1$ , we calculate OH content of  $\sim 0.25\text{--}0.35$  p.f.u., within the range of measured mare basalt apatites [7].

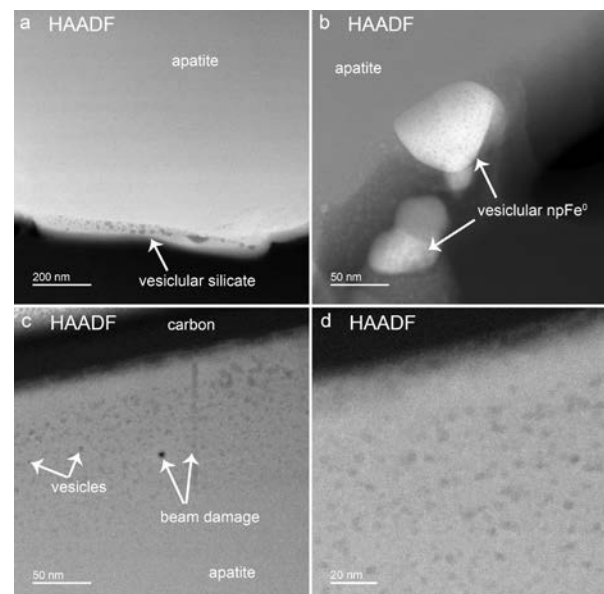


**Figure 2.** HAADF images of various rim features on the apatite including (a) a vesicular,  $\text{npFe}^0$ -rich silicate rim on the apatite, (b) several vesicular  $\text{npFe}^0$  particles on the surface of the apatite, and (c,d) a vesicular rim in the apatite.

The bottom shows little evidence of alteration to the apatite itself, but portions are coated in vesicular,  $\text{npFe}^0$ -rich silicate glass, most likely a melt splash (Fig. 2a). A vesicular  $\text{npFe}^0$  particle is also attached to the surface and contains a small amount of He (Fig. 2b).

Most of the top surface of the sample has a crystalline, vesicular rim with small (2-5 nm) vesicles covered by a thin, poorly crystalline, vesicle-free layer of apatite composition (Fig. 2c,d). The vesicles extend to a depth of ~100 nm. There is a slight decrease in P in the poorly crystalline material, but no difference in composition between the vesicular rim and deeper material.

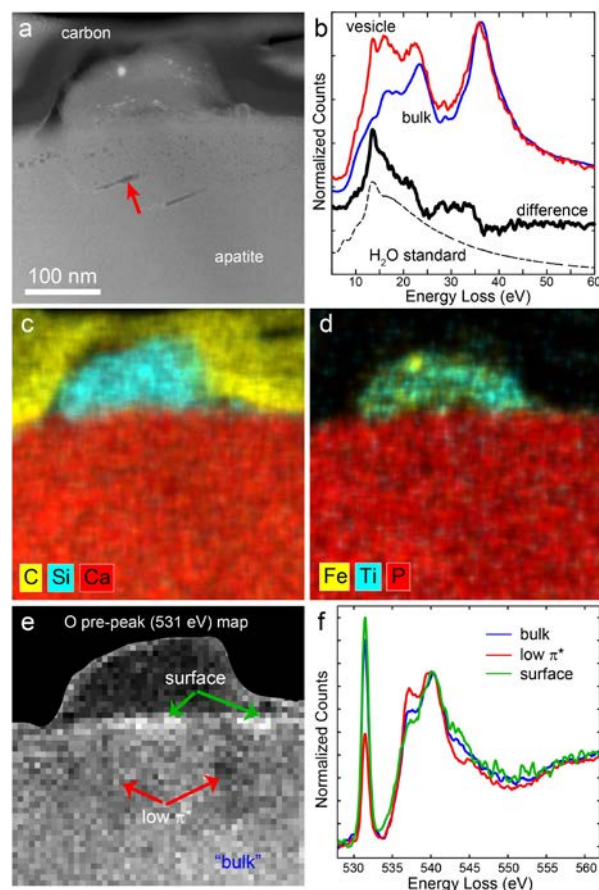


**Figure 3.** (a) HAADF image of surface of apatite grain showing large and small vesicles beneath a Si-rich glassy bleb. (b) EELS spectra from “bulk” apatite (blue) and vesicle noted by red arrow in (a) (red). A difference spectrum (black) shows the distinct peak at ~13 eV and general shape of water in the vesicle. Standard from [8]. (c,d) EDS maps show glassy bleb on apatite with no compositional changes in vesicle-rich rim. (e) Map of the 531 eV oxygen  $\pi^*$  peak normalized by the signal at 540 eV. (f) O-K EELS spectra from several regions in the rim showing variation in pre-peak height and peak shape.

Within the vesicular rim, there are several larger, elongate (possibly planar) vesicles (Fig. 3a). These large vesicles, which are parallel to each other and may indicate crystallographic control of their orientation, sit 80-100 nm below the apatite surface, directly beneath a

glassy silicate bleb of variable composition that contains  $\text{npFe}^0$  and nano-sulfides. The EELS signal for one of these vesicles shows the clear presence of water within the vesicle (Fig. 3b). Principal component analysis (PCA) and/or non-linear least squares fitting of potential end-members suggests some water signal is present in many vesicles to lesser degrees based on elevated signal in the 10-20 eV region compared to surrounding material.

Oxygen K-edge EELS shows a pre-peak at ~531 eV that is highly variable in height relative to the main edge across the rim (Fig. 3e,f). The  $\pi^*$  pre-peak, suggestive of the presence of  $\text{O}_2$  or oxygen radicals caused by radiation damage from the electron beam or possibly the solar wind itself [9,10], is less pronounced within the water-containing vesicle than the surrounding rim material. Other portions of the apatite away from this rim show little to no pre-peak.

The position of the large vesicles directly beneath the melt bleb but not in other sections of the rim suggests heating contributed to their development. Basic thermodynamic calculations show this region could have been above the temperature at which OH becomes mobile in the apatite lattice for several seconds [11], so the water detected in the vesicles could be from a combination of solar wind and lattice water.

**Conclusions:** The clear presence of water trapped in vesicles in a lunar apatite grain is the first unequivocal measurement of such in a lunar space weathered rim. Because water is incorporated in the apatite crystal structure, it is possible that some water is in fact from dehydrogenation during heating rather than from the solar wind, although vesicles are seen only in the rim. The stability of water in the apatite structure relative to the main anhydrous lunar silicates may also affect its ability to retain water in vesicles after their formation.

**Acknowledgments:** This work was supported by NASA through an ANGSA program award to KDB and SSERVI RISE2.

**References:** [1] Robinson, K.L., and Taylor, G.J. (2014) *Nat Geosci*, 7, 401. [2] Keller, L.P., and McKay, D.S. (1997) *Geochim Cosmochim Acta*, 61, 2331. [3] Bradley, J.P., et al. (2014) *Proc Nat Acad Sci*, 111, 1732. [4] Burgess, K.D., and Stroud, R.M. (2018) *Geochim Cosmochim Acta*, 224, 64. [5] Anand, M., et al. (2012) *Planet Space Sci*, 74, 42. [6] Benna, M., et al. (2019) *Nat Geosci*, 12, 333. [7] McCubbin, F.M., et al. (2015) *Am Mineral*, 100, 1790. [8] Cassidy, C., et al. (2017) *PLOS ONE*, 12, e0186899. [9] Ermi, R., et al. (2005) *Micron*, 36, 369. [10] Jiang, N., and Spence, J.C.H. (2006) *Ultramicroscopy*, 106, 215. [11] Tönsuaadu, K., et al. (2012) *J Therm Anal Calorim*, 110, 647.